

Segmentation of Cell Membrane and Nucleus using Branches with Different Roles in Deep Neural Network

Tomokazu Murata¹, Kazuhiro Hotta¹, Ayako Imanishi², Michiyuki Matsuda² and Kenta Terai²

¹Meijo University, 468-8502, Nagoya, Aichi, Japan

²Kyoto University, 606-8315, Kyoto, Japan

{ matsuda.michiyuki.2c, terai.kenta.5m } kyoto-u.ac.jp

Keywords: Segmentation, Cell Membrane, Cell Nucleus, Convolutional Neural Network, U-Net and Bioimage.

Abstract: We propose a segmentation method of cell membrane and nucleus by integrating branches with different roles in a deep neural network. When we use the U-net for segmentation of cell membrane and nucleus, the accuracy is not sufficient. It may be difficult to classify multi-classes by only one network. Thus, we designed a deep network with multiple branches that have different roles. We give each branch a role which segments only cell membrane or nucleus or background, and probability map is generated at each branch. Finally, the generated probability maps by three branches are fed into the convolution layer to improve the accuracy. The final convolutional layer calculates the posterior probability by integrating the probability maps of three branches. Experimental results show that our method improved the segmentation accuracy in comparison with the U-net.

1 INTRODUCTION

For the development of cell biology, it is important to understand the state of cells accurately. Currently, the most accurate way to check the state of cells is human visual inspection. However, it requires much time and effort. In addition, the results become subjective. Therefore, the automation of the process is desired in the field of cell biology. In this paper, we propose an automatic segmentation method of cell membrane and nucleus.

In recent years, deep learning gave high accuracy in many computer vision tasks (Tang and Wu, 2016, Tseng, Lin, Hsu, and Huang, 2017, Caesar, Uijlings and Ferrari, 2016, Ghiasi and Fowlkes, 2016). In particular, encoder-decoder CNN such as U-net (Ronneberger, Fischer and Brox, 2015) and Segnet (Badrinarayanan, Kendall and Cipolla, 2015) are recent trend of semantic segmentation. The advantage of U-net is to integrate the features at shallow layers and at deep layers, and features which are lost by convolution are used at deeper layers effectively. When we apply the U-net to segment cell membrane and nucleus, the accuracy is not sufficient for cell biologists. Since it is important to know how cell nucleus is covered by cell membranes, many

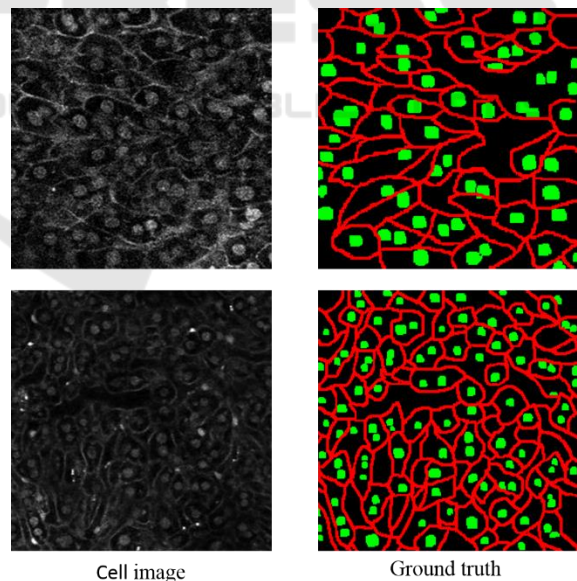


Figure 1: Example of cell images and ground truth labels. Red shows the cell membrane and green shows cell nucleus.

discontinuities of cell membranes are not good for biologists. It may be difficult to classify multi-classes by the standard U-net. In order to address this issue, we propose to give the U-net multiple branches for solving different roles.

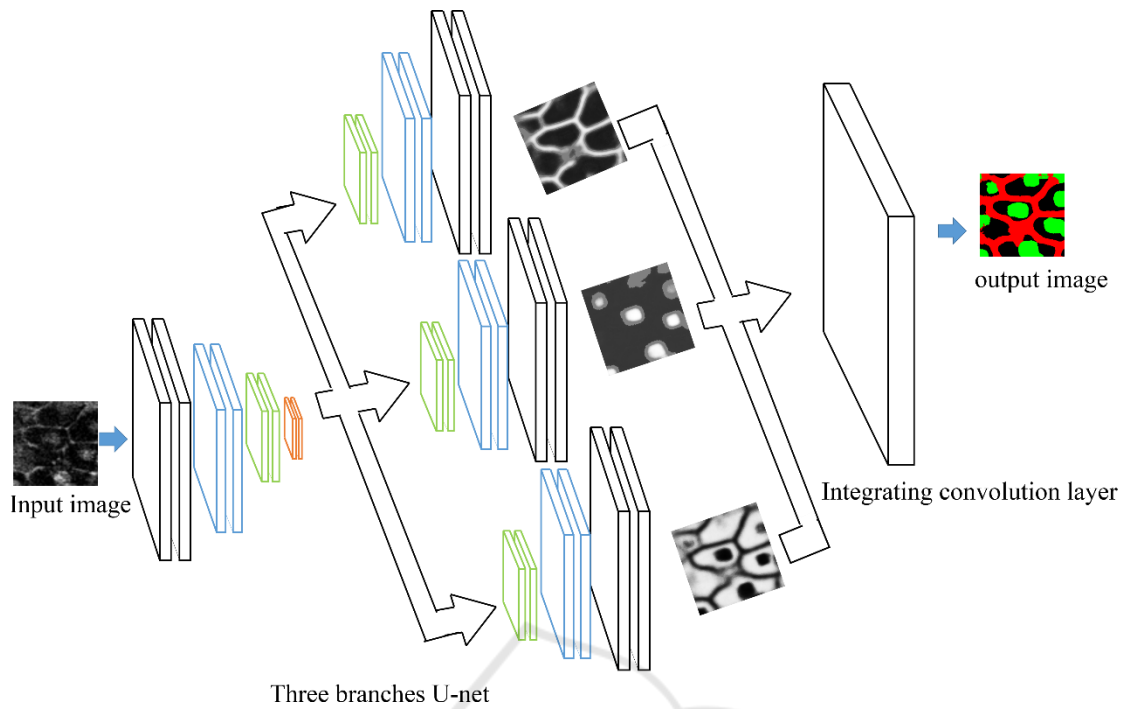


Figure 2: Overview of the proposed network. The decode part is divided into three parts, although all the branches are connected with the encoder parts and concatenated. This model optimized the output obtained by each branch and the result of integrating them with soft max cross entropy.

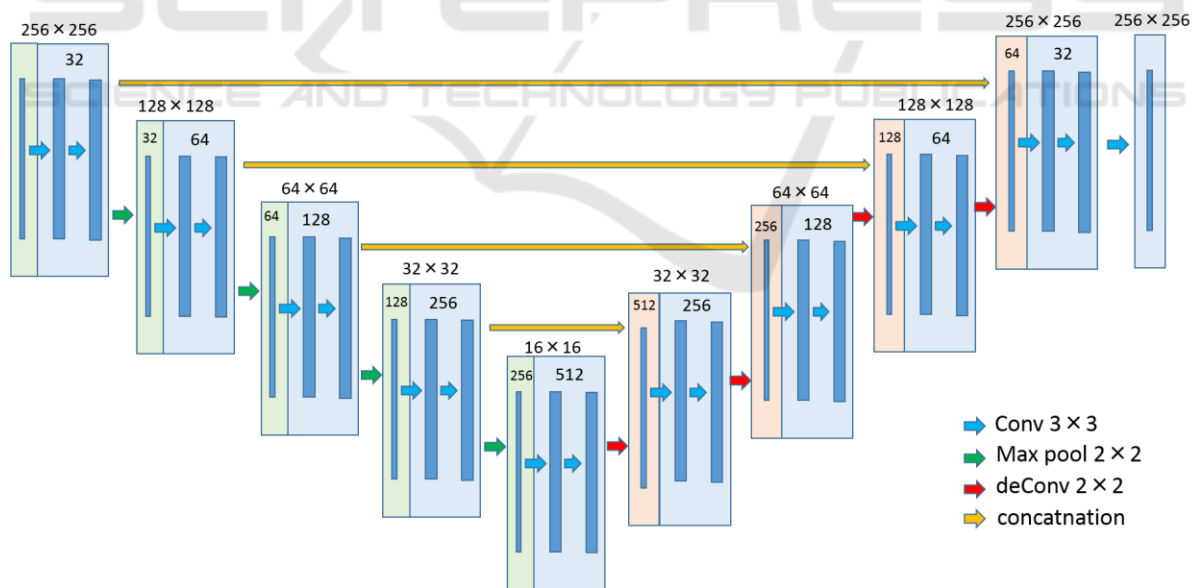


Figure 3: Structure of U-nets used in this paper. The number in the square shows the number of feature map.

In this paper, we use the network structure with reference to the U-net. The encoded part is the same structure as the original U-net, and we modified the decoder part of U-net. The decoder part is divided into three branches. Each branch has a unique role

that generates a probability map for cell nucleus or cell membrane or background from the feature maps obtained by encoder. Finally, single convolution layer combines the three probability maps, and it gives final segmentation result.

In the experiments, we used 50 fluorescence images of the liver of transgenic mice that expressed fluorescent markers on the cell membrane and in the nucleus. Figure 1 shows the examples of cell image and ground truth label attached by human experts. Input for the network is grayscale image and the output is 3 probability maps that each probability map is for cell membrane, nucleus and background. Red shows the cell membrane and green shows cell nucleus. We evaluated segmentation results by class-average accuracy, and we confirmed that our proposed method improved the accuracy of cell membrane or nucleus in comparison with the U-net.

This paper is organized as follows. In section 2, we explain the proposed method with different roles. Dataset and experimental results are shown in section 3. Comparison with conventional U-net is also shown. Section 4 is for conclusion and future works.

2 PROPOSED METHOD

Figure 2 and 3 show the overview of our proposed network and the structure of the U-net used in this paper. Input image is a grayscale image including cell membrane and nucleus. As described previously, it is difficult for simple U-net to segment cell membrane and nucleus simultaneously. Thus, we add branches to the decoder part of the U-net and assign each branch to different task. The outputs of three branches are integrated by a convolution layer to obtain the final segmentation result. This may be a kind of curriculum learning (Bengio, 2009). Three decoder parts try to do only one task, and the final convolution layer tries to integrate three branches.

At first, an input image is fed into encoder part of the U-net. Features are extracted by multiple convolutions and pooling. The encoded feature is fed into the three decoders with different roles. Each decoder learns to output the probability map for only cell membrane or nucleus or background.

Each branching decoder part calculates the probability of each pixel whether the certain class (e.g. cell nucleus) in 3 classes or not. Thus, the input of final convolutional layer is probability maps with 6 channels, and the output of it is the probability map for 3 classes; cell nucleus, cell membrane and background. We use softmax cross entropy as the losses for three branches and final integration layer.

In this paper, we use the weighted sum of losses of three decoders with different roles and integrated layer. The whole networks are trained simultaneously. The weighed loss is defined as

$$\text{Loss} = \sum_c \lambda_c L_c + \lambda_l L_l, \tag{1}$$

where c is the class that is one of cell nucleus, membrane and background. L_c is the loss generated by the c -th branch. L_l is the loss for the convolutional layer for final segmentation result. In experiments, we set those parameters as $\lambda_c = 0.2$, $\lambda_l = 0.4$ empirically.

Each loss is defined as

$$L_c = -\sum_i^n y_{ci} \log(S(x_{ci})), \tag{2}$$

$$L_l = -\sum_i^n \alpha_c y_{li} \log(S(x_{li})), \tag{3}$$

where x_{ci} , x_{li} are the output of three branches and final convolutional layer respectively. “ i ” means the i -th pixel in an input image, and y_{ci} and y_{li} are the ground truth. α_c is class-balancing weight (Badrinarayanan, Kendall and Cipolla, 2015). Class-balancing is a method for weighting the loss of each class according to the number of pixels in each class. In this paper, background pixels are overwhelmingly larger than the number of cell nucleus and membranes. Thus, the network tends to learn to background dominantly. By applying the weights according to occurrence of each class, all classes are trained equally. In this paper, the class weights of cell membrane, cell nucleus and background are 1, 2.72 and 0.42, respectively.

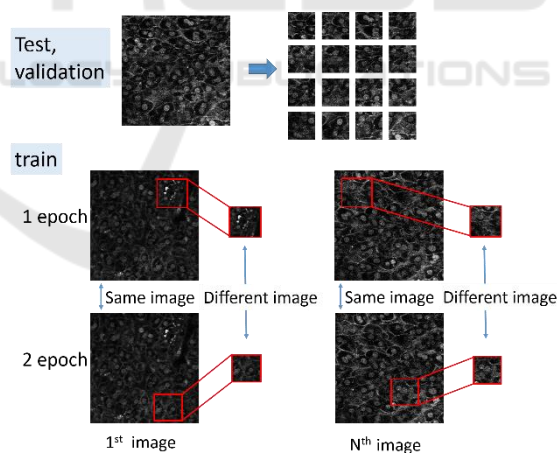


Figure 4: Cropping local region. At every epoch, different images are cropped from training images. This prevents overfitting.

3 EXPERIMENTS

This section explains the dataset, evaluation measure and results. In section 3.1, we describe the dataset used in this paper. Evaluation measure is also

explained in section 3.1. Experimental results are shown in section 3.2. Comparison result with the U-net is also shown.

3.1 Dataset and Evaluation Measure

We use original dataset which includes fluorescence images of the liver of transgenic mice that expressed fluorescent markers on the cell membrane and in the nucleus. To train the segmentation network, we require fluorescence images with ground truth. However, creating ground truth labels for cell images is a labor job for cell biologists. Therefore, the number of images with ground truth is limited. In this paper, we have only 50 images. The size of those images is 256 x 256 pixels. Examples of cell images and ground truth labels are shown in Figure 1. Red and green show the cell membrane and nucleus. In the following experiments, 50 images are divided into three sets; 35 training images, 5 validation images and 10 test images.

To solve the problem on a small number of images, data augmentation of training images is used. Concretely, left-right mirroring and rotations with 90 degrees are combined, and the number of training images is 8 times larger. In addition, we crop local regions with 64 x 64 pixels from the augmented images randomly. Since the size of input images for the U-net is 256 x 256 pixels, the cropped images are resized to 256 x 256 pixels and used for training.

To prevent the overfitting, we crop local regions randomly at each epoch when we train the network. Figure 4 shows the overview of this process. Since different local regions with ground truth are cropped randomly at each epoch from training images, the network can avoid the overfit.

When we evaluate test images, a test image with 256 x 256 pixels is divided into 4 x 4 without overlap. The cropped 64 x 64 images are resized to 256 x 256 pixels and fed into the proposed method. By this processing, the number of images used for the final test is 160 and the number of validation is 80.

In experiments, we use class average accuracy as the evaluation measure because the main purpose of this research is to segment cell membrane and nucleus. Since the area of background is the largest, pixel-wise accuracy heavy depends on the accuracy of background. On the other hand, since class average accuracy is the average of accuracy of each class, the accuracy of small area is influenced to the class average accuracy.

Since the accuracy of deep learning depends on the random number, we trained the networks three times and evaluate the average accuracy.

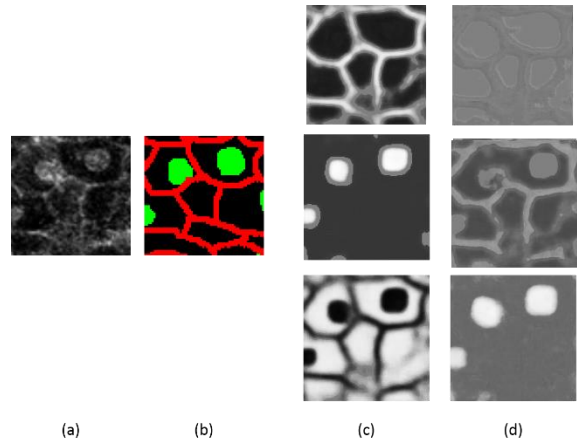


Figure 5: Comparison of output of no weight branches U-nets. (a) shows a test local region. (b) shows ground truth. (c) shows the outputs by three branched decoder parts of U-net in the proposed method. (d) is the output of the network with the same structure as the proposed method when we do not give a role branched decoder parts of U-net.

3.2 Evaluation Results

To show the effectiveness of the proposed method integrating three branches with different roles, we also evaluate the network with the same structure as the proposed method as shown in Figure 2. But we evaluated the proposed method while changing the value of λ . One of them is $\lambda_c = 0$, $\lambda_l = 1$. Namely, this optimizes only the cross entropy loss at the final output. By the comparison with this network, we understand the effectiveness of training of three branches with different roles. Of course, the accuracy of the U-net as shown in Figure 3 is also evaluated.

Table 1 shows the accuracy of each method. As described previously, we trained each method three times and average accuracy is evaluated because the accuracy of networks depends on random number. In this paper, each pixel in an input image is classified into three classes; cell membrane, cell nucleus and background. Table 1 shows that the accuracy changes slightly depending on the random number.

The mean accuracy of three time evaluation is shown in Table 2. We see that the accuracy of the proposed method outperformed with the U-net.

We also evaluate the network with the same structure as the proposed method and without giving a role to the branches. We see that the accuracy is worse than our proposed method.

Figure 5 shows the outputs of three branches in the proposed method and those in the network without specific roles. (a) and (b) show a test local region and its ground truth label. (c) and (d) show the outputs of the branched decoder part in both methods.

Table 1: Accuracy at three times evaluation.

| | proposed method ($\lambda_c=0.2, \lambda_l=0.4$) | | | proposed method ($\lambda_c=0.25, \lambda_l=0.25$) | | | proposed method ($\lambda_c=0.1, \lambda_l=0.7$) | | | proposed method ($\lambda_c=0, \lambda_l=1.0$) | | | U-net | | |
|---------------|---|-------|-------|---|-------|-------|---|-------|-------|---|-------|-------|-------|-------|-------|
| | 1st | 2nd | 3rd | 1st | 2nd | 3rd | 1st | 2nd | 3rd | 1st | 2nd | 3rd | 1st | 2nd | 3rd |
| cell membrane | 80.33 | 81.05 | 80.96 | 82.32 | 79.43 | 80.51 | 81.59 | 80.97 | 80.87 | 80.72 | 79.78 | 80.88 | 79.65 | 80.64 | 80.42 |
| cell nucleus | 89.88 | 89.63 | 87.58 | 88.69 | 88.70 | 87.45 | 88.96 | 87.50 | 87.03 | 86.80 | 87.70 | 85.49 | 84.94 | 87.65 | 88.87 |
| background | 64.52 | 63.63 | 65.06 | 63.30 | 66.01 | 66.03 | 62.81 | 65.51 | 65.86 | 64.82 | 65.74 | 65.06 | 65.24 | 64.80 | 64.80 |
| class-average | 78.25 | 78.11 | 77.87 | 78.10 | 78.05 | 78.00 | 77.78 | 77.99 | 77.92 | 77.45 | 77.74 | 77.14 | 76.61 | 77.64 | 77.97 |

Table 2: Average accuracy of three times evaluation.

| | proposed method ($\lambda_c=0.2, \lambda_l=0.4$) | proposed method ($\lambda_c=0.25, \lambda_l=0.25$) | proposed method ($\lambda_c=0.1, \lambda_l=0.7$) | proposed method ($\lambda_c=0, \lambda_l=1.0$) | U-net |
|---------------|---|---|---|---|-------|
| cell membrane | 80.78 | 80.75 | 81.14 | 80.46 | 80.24 |
| cell nucleus | 89.03 | 88.28 | 87.83 | 86.66 | 87.15 |
| background | 64.40 | 65.11 | 64.73 | 65.21 | 64.88 |
| class-average | 78.08 | 78.05 | 77.90 | 77.44 | 77.41 |

The proposed method gave obviously better maps than the network without a specific role. This result demonstrated that the integration of networks with specific role is effective to improve the accuracy.

(d) is the result that we trained the network without calculating the losses at the three branches. We conducted experiments three times under the same conditions, but similar results are obtained that one of the three branches had the function of focusing on the segment of the cell nucleus. In this paper, we give each clear role to three branches, but we found that this network has a little ability to share the roles automatically.

Finally, we show the segmentation results by the proposed method in Figure 6. Figure 6 (a) and (b) show the test images and their ground truth labels. (c) shows the results by the proposed method. We see that overall segmentation is good though the cell membrane is conspicuous. Figure 7 shows the segmentation results of local regions by the proposed method ($\lambda_c=0.2, \lambda_l=0.4$) and the U-net.

Figure (a) and (b) are the test local regions and their ground truth labels. (c) is the results by the proposed method. (d) is the results by the U-net. We see that the segmentation accuracy of cell membrane and nucleus is improved in comparison with the U-net.

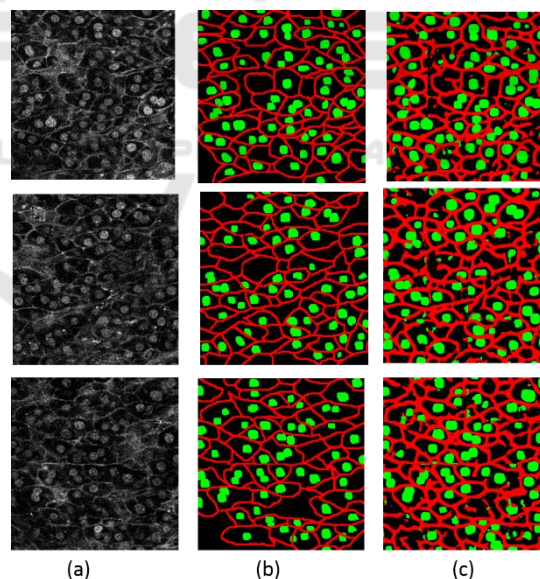


Figure 6: (a) shows test images. (b) shows ground truth. (c) shows the results by the proposed method.

In the results shown in the first and second row, there is a case that cell membranes disconnected by U-net are connected by the proposed method. The effectiveness of branches with different roles is demonstrated by experiments.

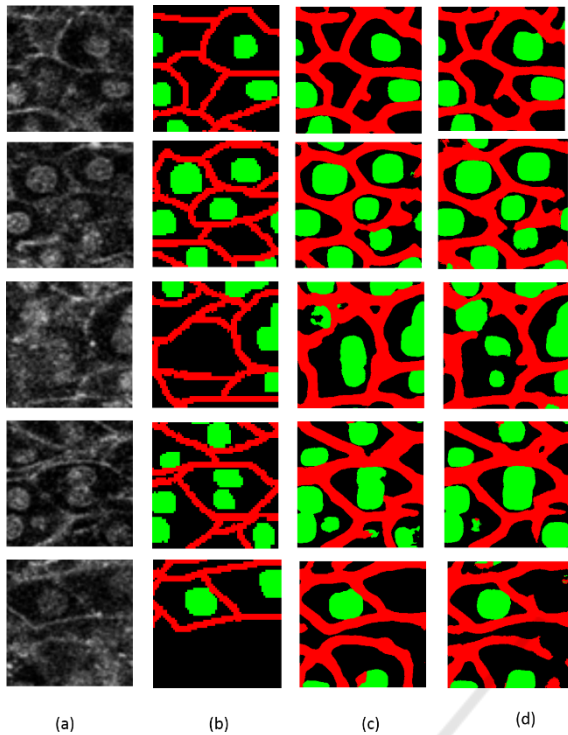


Figure 7: comparison results of local regions. (a) shows test regions. (b) shows ground truth. (c) shows the results by the proposed method using three branches. (d) shows the results by the U-net.

4 CONCLUSIONS

We improved the segmentation accuracy by using branches with different roles and final convolution layer. Three branches segment only cell membrane or nucleus or background, and the final convolution layer for integrating the outputs of three branches estimate the posterior probability of each pixel. By assigning each branched decoder to a different role, the accuracy was improved.

We crop a local region with 64×64 pixels from a test image without overlap, and the output of the local region is put to final segmentation result. If we apply the proposed method to local regions with overlapping manner, some segmentation results are obtained at the same pixel. The integration of those results will improve the accuracy further. It is a subject for future works.

ACKNOWLEDGEMENTS

This work is partially supported by MEXT/JSPS KAKENHI Grant Number 16H01435"Resonance Bio".

REFERENCES

- Ronneberger, O., Fischer, P., and Brox, T., 2015. U-net: Convolutional networks for biomedical image segmentation. In *International Conference on Medical Image Computing and Computer-Assisted Intervention* (pp. 234-241). Springer, Cham.
- Tang, Y., and Wu, X., 2016. Saliency detection via combining region-level and pixel-level predictions with cnns. In *European Conference on Computer Vision* (pp. 809-825). Springer International Publishing.
- Tseng, K. L., Lin, Y. L., Hsu, W., and Huang, C. Y., 2017. Joint Sequence Learning and Cross-Modality Convolution for 3D Biomedical Segmentation. *arXiv preprint arXiv:1704.07754*.
- Caesar, H., Uijlings, J., and Ferrari, V., 2016. Region-based semantic segmentation with end-to-end training. In *European Conference on Computer Vision* (pp. 381-397). Springer International Publishing.
- Ghiasi, G., and Fowlkes, C. C., 2016. Laplacian pyramid reconstruction and refinement for semantic segmentation. In *European Conference on Computer Vision* (pp. 519-534). Springer International Publishing.
- Badrinarayanan, V., Kendall, A., and Cipolla, R., 2015. Segnet: A deep convolutional encoder-decoder architecture for image segmentation. *arXiv preprint arXiv:1511.00561*.
- Bengio, Y., 2009. Learning deep architectures for AI. *Foundations and trends in Machine Learning*, 2(1), 1-127.